JOURNAL OF MATERIALS SCIENCE **38** (2003) 4365–4371

On strain localization in the high rate extension of nylon fibers

T. A. GODFREY
Natick Soldier Center, US Army Soldier & Biological Chemical Command, Natick, Massachusetts 01760-5020, USA
E-mail: godfreyt@natick.army.mil

A simple analytical model for the adiabatic high strain rate extension of synthetic textile fibers is presented. The model suggests that, for fibers with particular thermo-mechanical and constitutive properties, initial nominally uniform strain distributions along the fiber will tend to become non-uniform, with localization of axial strain into a thermally softened region. To assess the usefulness of the model in predicting and interpreting fiber behavior, a commercial nylon filament is investigated experimentally. Nylon filaments are extended to break at a low, isothermal strain rate (0.0015 s^{-1}) and at a high, adiabatic strain rate (70 s^{-1}). A dimensionless *strain localization parameter* (SLP), used to characterize the nylon filament in the framework of the model, predicts strain localization to occur during extension at the 70 s^{-1} strain rate. Experimental load-extension curves exhibit a sharply reduced elongation-to-break at the high strain rate, consistent with the predicted occurrence of localized, versus uniform, straining. In addition, the transition from homogeneous to localized straining appears to occur at elongations that correspond with the SLP attaining a critical value for onset of localization.

1. Introduction

It is well known among fiber and textile scientists that when certain synthetic fibers are extended to failure at high-strain rates, the broken ends exhibit signs of melting. When this phenomenon was first discussed in the 1950's [1], researchers realized that the observed melting could only occur if a significant fraction of the work done in extending the fiber to break was dissipated locally around the site of the eventual rupture. At that time, the specific mechanism through which such localization of energy dissipation would occur was unclear. Now, of course, strain localization and material instability phenomena are well known, and it is natural to consider the possibility that the melting seen in high rate fiber extension tests is associated with the final stages of a strain localization process involving thermal softening.

This paper is concerned with the role of thermo-mechanical coupling in the extension process, where the energy and momentum balance in the extending filament are tightly coupled through the temperature dependence of the filament's constitutive law. Generally, the mechanical behavior of polymeric materials is highly sensitive to temperature, so modeling and understanding the effects of thermo-mechanical coupling is an important research area. For a brief review of the literature concerning thermo-mechanical coupling in the mechanics of polymeric materials, particularly works relevant to fibers, readers may refer to reference [2].

In the present work, we generalize a simple analytical model [2] for the stability of homogeneous straining motion in the high-rate extension of textile filaments to treat a broad class of filaments exhibiting nonlinear plastic load-strain behavior. Extension experiments on a commercial nylon filament at a low and a high nominal strain rate are presented, and the model is used to interpret the experiments. The nylon filament's high-rate behavior is characterized using a dimensionless *strain localization parameter* (SLP) that arises from the model. The SLP is regarded as a function of the nylon filament's elongation and estimates are presented indicating the onset of strain localization in high-rate extension at elongations of roughly 0.23–0.27. The experiments show a significantly reduced elongation-to-break for the high-strain rate tests—consistent with the predicted occurrence of localized, versus uniform, straining. Elongations-to-break in the high-rate tests are in the same range as the predicted elongations for onset of strain localization.

2. Mathematical model

In this section, we summarize and extend a mathematical model originally introduced in [2]. In the development given here, the model is generalized to treat fibers with nonlinear plastic load-strain behavior.

2.1. Constitutive model

In reference [2], a simple constitutive model was used for the fiber's plastic load-strain-temperature behavior, where it was assumed that the isothermal plastic

load-strain curve was linear. Here we reinterpret the earlier model to apply broadly to fibers exhibiting nonlinear behavior. Consider the extension of a textile fiber. Fiber behavior is elastic up to a yield point, beyond which the fiber is plastically deformed. Our concern is with the plastic extension of the fiber, and we restrict our attention to the case where plastic strain is monotonically increasing with time, i.e., the fiber does not anywhere experience elastic unloading. The tension, p, carried by the fiber is a function of axial strain, ε, temperature, T, and axial strain rate, $\dot{\varepsilon}$, i.e., $p = f(\varepsilon, T, \dot{\varepsilon})$. Expanding in a Taylor series to the first order, the fiber tension is written as,

$$p \cong f(\varepsilon_0, T_0, \dot{\varepsilon}_0) + f_\varepsilon(\varepsilon_0, T_0, \dot{\varepsilon}_0)(\varepsilon - \varepsilon_0) + f_T(\varepsilon_0, T_0, \dot{\varepsilon}_0)(T - T_0) + f_{\dot{\varepsilon}}(\varepsilon_0, T_0, \dot{\varepsilon}_0)(\dot{\varepsilon} - \dot{\varepsilon}_0) \quad (1)$$

where $\varepsilon > \varepsilon_0$, variable subscripts denote partial differentiation with respect to that variable, and the subscript 0 denotes an arbitrary point in the process of plastically extending the filament. Experimental results indicate a logarithmic dependence of the plastic load on strain rate [3], therefore we may neglect the term involving the first partial with respect to $\dot{\varepsilon}$ in Equation 1. In the analysis to follow, we will investigate the stability of homogeneous straining motion of the fiber at an arbitrary point in the extension process. Our constitutive model need only represent a short duration of the filament extension from the arbitrary point under consideration. Introduce a dimensionless temperature $\theta = (T - T_0)/T_0$, and denote $f(\varepsilon_0, T_0, \dot{\varepsilon}_0)$ as p_0. Equation 1 is rewritten as,

$$p \cong p_0 - a\theta + b\varepsilon^*, \quad (2)$$

where a is the thermal softening coefficient ($a = -f_T(\varepsilon_0, T_0, \dot{\varepsilon}_0)T_0$), b is the strain hardening coefficient ($b = f_\varepsilon(\varepsilon_0, T_0, \dot{\varepsilon}_0)$), and $\varepsilon^* = \varepsilon - \varepsilon_0$.

2.2. Equations of motion and energy balance

Consider a fiber of length, l, density, ρ, and cross-sectional area, A, held fixed at its end at $x = 0$ and being extended by the motion of the end at $x = l$ at constant velocity $\dot{\varepsilon}_0 l$. The nominal rate of strain, $\dot{\varepsilon}_0$, is sufficiently high such that adiabatic conditions apply and the fiber is assumed to be fully plastic. We investigate the motion of the fiber for a short duration beginning at an arbitrary instant in time, $t = 0$. Introduce $u(x, t)$ as the x displacement of points on the fiber, where the displacement reference is the position of points on the fiber at $t = 0$. The equation of motion for a differential element of the fiber, length $\mathrm{d}x$, mass $\rho A \mathrm{d}x$, may be written by considering the balance of forces, Fig. 1, as

$$\rho A \frac{\partial^2 u}{\partial t^2} = -a\frac{\partial \theta}{\partial x} + b\frac{\partial^2 u}{\partial x^2}, \quad (3)$$

where we make use of Equation 2, and the fact that $\varepsilon^* = \partial u/\partial x$.

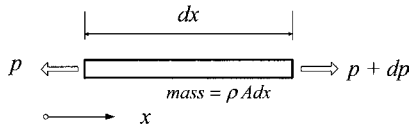

Figure 1 Dynamic force balance on differential element of fiber.

The portion of plastic work done on the differential element of the fiber that is dissipated as heat raises the thermal energy of the element. The remaining portion of the plastic work done increases the internal energy of the fiber element through structure changes, such as increased molecular orientation. Forming the energy balance, the time rate of change of thermal energy of the element is equal to the rate at which plastic work is dissipated in the element. The specific heat of the fiber material is c and the fraction of plastic work that is dissipated as heat is η. The rate of change of thermal energy in the element is $\rho c A \mathrm{d}x \partial T/\partial t$ and the rate of energy dissipation in the element is $\eta p \dot{\varepsilon}^* \mathrm{d}x$. Using Equation 2, the definition of dimensionless temperature, θ, and that $\dot{\varepsilon}^* = \partial^2 u/\partial t \partial x$, the energy balance may be written as

$$\rho c A T_0 \frac{\partial \theta}{\partial t} = \eta\left(p_0 - a\theta + b\frac{\partial u}{\partial x}\right)\frac{\partial^2 u}{\partial t \partial x} \quad (4)$$

Displacement boundary conditions at the fiber's ends for constant rate extension are

$$u(0, t) = 0, \quad u(l, t) = \dot{\varepsilon}_0 l t \quad (5)$$

Homogeneous straining deformation of the fiber, $\varepsilon^*(x, t) = \dot{\varepsilon}_0 t$, results in a displacement field written as

$$u(x, t) = \dot{\varepsilon}_0 x t. \quad (6)$$

Dimensionless position, x^*, and time, t^*, coordinates are defined as

$$x = l x^*, \quad t = \frac{\rho c A T_0}{\eta a \dot{\varepsilon}_0} t^*, \quad (7)$$

and a dimensionless displacement, U, is defined as

$$u = l U \quad (8)$$

Substitution of Equations 7 and 8 into 3 and 4 gives the following dimensionless equation of motion and equation of energy balance

$$\frac{\partial^2 U}{\partial t^{*2}} + \frac{\rho A c^2 T_0^2}{\eta^2 a \dot{\varepsilon}_0^2 l^2}\left(\frac{\partial \theta}{\partial x^*} - \frac{b}{a}\frac{\partial^2 U}{\partial x^{*2}}\right) = 0 \quad (9)$$

and

$$\frac{\partial \theta}{\partial t^*} = \frac{\eta}{\rho c A T_0}\left(p_0 - a\theta + b\frac{\partial U}{\partial x^*}\right)\frac{\partial^2 U}{\partial t^* \partial x^*}, \quad (10)$$

respectively.

2.3. Stability analysis

Our aim is to investigate the stability of homogeneous straining deformation by considering the dynamic response to small disturbances in the velocity field along

the fiber. In this regard, the dimensionless displacement and temperature are considered the sum of the homogeneous straining response and a small perturbation due to an initial disturbance at $t^* = 0$. Introduce perturbed displacement and temperature variables,

$$\begin{aligned} U(x^*, t^*) &= U_{\mathrm{HS}}(x^*, t^*) + \bar{U}(x^*, t^*), \\ \theta(x^*, t^*) &= \theta_{\mathrm{HS}}(t^*) + \bar{\theta}(x^*, t^*) \end{aligned} \tag{11}$$

where subscripts *HS* denote the homogeneous straining response and over-bars indicate the small perturbation. The dimensionless homogeneous straining displacement may be written, using Equations 6–8, as,

$$U_{\mathrm{HS}} = \frac{\rho c A T_0}{\eta a} x^* t^* \tag{12}$$

Substituting Equations 11 and 12 into 9, we obtain an equation in the perturbed variables, written as,

$$\frac{\partial^2 \bar{U}}{\partial t^{*^2}} + \frac{\rho A c^2 T_0^2}{\eta^2 a \dot{\varepsilon}_0^2 l^2} \left(\frac{\partial \bar{\theta}}{\partial x^*} - \frac{b}{a} \frac{\partial^2 \bar{U}}{\partial x^{*^2}} \right) = 0 \tag{13}$$

Making the substitution of Equations 11 and 12 into 10, we obtain

$$\begin{aligned} \frac{\mathrm{d}\theta_{\mathrm{HS}}}{\mathrm{d}t^*} + \frac{\partial \bar{\theta}}{\partial t^*} = \frac{\eta}{\rho c A T_0} \Bigg(& p_0 - a\theta_{\mathrm{HS}} - a\bar{\theta} + b \frac{\rho c A T_0}{\eta a} t^* \\ & + b \frac{\partial \bar{U}}{\partial x^*} \Bigg) \left(\frac{\rho c A T_0}{\eta a} + \frac{\partial^2 \bar{U}}{\partial t^* \partial x^*} \right) \end{aligned} \tag{14}$$

By neglecting terms in Equation 14 involving the perturbations, an ordinary differential equation for θ_{HS} may be obtained,

$$\frac{\mathrm{d}\theta_{\mathrm{HS}}}{\mathrm{d}t^*} + \theta_{\mathrm{HS}} = \frac{p_0}{a} + \frac{b \rho c A T_0}{\eta a^2} t^* \tag{15}$$

Subtracting (15) from (14), an equation for the perturbations is obtained,

$$\begin{aligned} & \frac{\partial \bar{\theta}}{\partial t^*} + \bar{\theta} - \frac{b}{a} \frac{\partial \bar{U}}{\partial x^*} - \left(\frac{\eta p_0}{\rho c A T_0} - \frac{\eta a}{\rho c A T_0} \theta_{\mathrm{HS}} + \frac{b}{a} t^* \right) \\ & \times \frac{\partial^2 \bar{U}}{\partial t^* \partial x^*} \cong 0 \end{aligned} \tag{16}$$

where small terms involving products of perturbations have been neglected.

We consider the stability of uniform straining at an arbitrary point in the extension process. At this arbitrary point, the fiber temperature is T_0. Therefore, the initial condition on θ_{HS} is $\theta_{\mathrm{HS}}(0) = 0$. With this condition, Equation 15 may be integrated to obtain

$$\begin{aligned} \theta_{\mathrm{HS}} = & \left(\frac{b \rho c A T_0}{\eta a^2} - \frac{p_0}{a} \right) e^{-t^*} - \left(\frac{b \rho c A T_0}{\eta a^2} - \frac{p_0}{a} \right) \\ & + \frac{b \rho c A T_0}{\eta a^2} t^*. \end{aligned} \tag{17}$$

Equation 17 may be substituted into Equation 16 to obtain an equation containing only the perturbed variables, written as

$$\begin{aligned} & \frac{\partial \bar{\theta}}{\partial t^*} + \bar{\theta} - \frac{b}{a} \frac{\partial \bar{U}}{\partial x^*} \\ & - \left\{ \left(\frac{\eta p_0}{\rho c A T_0} - \frac{b}{a} \right) e^{-\mathrm{t}^*} + \frac{b}{a} \right\} \frac{\partial^2 \bar{U}}{\partial t^* \partial x^*} \cong 0. \end{aligned} \tag{18}$$

Equations 13 and 18 represent the dynamic behavior of small motions in the neighborhood of the uniform straining of the fiber with nominal strain rate $\dot{\varepsilon}_0$. The stability of the homogeneous straining motion *in the small* may be investigated by exploring the nature of the solutions to the coupled equations given small initial disturbances.

The perturbed variables are expressed as Fourier sine and cosine series expansions, written as

$$\bar{U}(x^*, t^*) = \sum_{n=1}^{\infty} r_{\mathrm{n}}(t^*) \sin(n\pi x^*) \quad \text{and}$$

$$\bar{\theta}(x^*, t^*) = \sum_{n=1}^{\infty} q_{\mathrm{n}}(t^*) \cos(n\pi x^*).$$

The sine series expansion selected for $\bar{U}$ satisfies boundary conditions on the perturbed displacement, $\bar{U}(0, t^*) = \bar{U}(1, t^*) = 0$. Substituting the Fourier expansions into Equations 13 and 18, we obtain two ordinary differential equations in the unknown functions of time, $r_{\mathrm{n}}(t^*)$ and $q_{\mathrm{n}}(t^*)$. Using linear operator notation, q_{n} and it's derivatives may be eliminated to obtain a single third-order equation in r_{n}, written as

$$r_{\mathrm{n}} + \ddot{r}_{\mathrm{n}} - n^2 \pi^2 \frac{\rho A c^2 T_0^2 b}{\eta^2 a^2 \dot{\varepsilon}_0^2 l^2} \left\{ \frac{a \eta p_0}{b \rho c A T_0} - 1 \right\} e^{-t^*} \dot{r}_{\mathrm{n}} \cong 0 \tag{19}$$

where over-dots denote $\frac{\mathrm{d}}{\mathrm{d}t^*}(\ )$. Equation 19 may be regarded as a second-order equation in the unknown functions, $\dot{r}_{\mathrm{n}}(t^*)$, forming the coefficients of a Fourier sine series expansion of the perturbed velocity field, $\partial \bar{U} / \partial t^*$.

A solution involving modified Bessel functions may be obtained for Equation 19 through a change of variables. Introduce a new independent variable, $z = e^{-\mathrm{t}^*}$, and dependent variable, $w_{\mathrm{n}} = \dot{r}_{\mathrm{n}}$. Substituting these into Equation 19, computing the indicated derivatives, gives the following second-order equation in $w_{\mathrm{n}}(z)$

$$z^2 w_{\mathrm{n}}'' - z k_{\mathrm{n}} w_{\mathrm{n}} = 0 \tag{20}$$

where $(\ )' = \frac{\mathrm{d}}{\mathrm{d}z}(\ )$ and $k_{\mathrm{n}} = n^2 \pi^2 \frac{\rho A c^2 T_0^2 b}{\eta^2 a^2 \dot{\varepsilon}_0^2 l^2} \{ \frac{a \eta p_0}{b \rho c A T_0} - 1 \}$. The general solution to Equation 20 may be written as

$$w_{\mathrm{n}}(z) = B_{\mathrm{n}} \sqrt{z} I_1(2\sqrt{k_{\mathrm{n}} z}) + C_{\mathrm{n}} \sqrt{z} K_1(2\sqrt{k_{\mathrm{n}} z}) \tag{21}$$

where I_1 and K_1 are modified Bessel functions of first and second kinds of order one, and B_{n} and C_{n} are integration constants.

Consider an initial slight disturbance in the velocity field. The coefficients in a Fourier sine series expansion of the disturbance are δ_n. Therefore, initial conditions on $\dot{r}_n(t^*)$ are $\dot{r}_n(0) = \delta_n$ and $\ddot{r}_n(0) = 0$. In the new variables, the initial conditions become $w_n(1) = \delta_n$ and $w_n'(1) = 0$. Evaluation of the integration constants in Equation 21 to satisfy the aforementioned initial conditions gives

$$\frac{B_n}{\delta_n} = \frac{K_0(2\sqrt{k_n}) - k_n^{-1/2}K_1(2\sqrt{k_n}) + K_2(2\sqrt{k_n})}{I_0(2\sqrt{k_n})K_1(2\sqrt{k_n}) + I_1(2\sqrt{k_n})K_0(2\sqrt{k_n}) + I_1(2\sqrt{k_n})K_2(2\sqrt{k_n}) + I_2(2\sqrt{k_n})K_1(2\sqrt{k_n})}, \tag{22a}$$

and

$$\frac{C_n}{\delta_n} = \frac{I_0(2\sqrt{k_n}) + k_n^{-1/2}I_1(2\sqrt{k_n}) + I_2(2\sqrt{k_n})}{I_0(2\sqrt{k_n})K_1(2\sqrt{k_n}) + I_1(2\sqrt{k_n})K_0(2\sqrt{k_n}) + I_1(2\sqrt{k_n})K_2(2\sqrt{k_n}) + I_2(2\sqrt{k_n})K_1(2\sqrt{k_n})} \tag{22b}$$

where the I's and K's are modified Bessel functions of the first and second kind, respectively, of the order indicated by the subscript. We consider the evolution of the perturbed velocity field with time by substituting Equations 22a and b into Equation 21, and replacing z with e^{-t^*}. For negative values of k_n, which occur for values of the parameter $a\eta p_0/b\rho cAT_0$ less than one, the components of the perturbed velocity field are found to decay, with some oscillation, reaching stationary values less than their initial values, δ_n. In this case, since any component of the Fourier expansion of the initial velocity disturbance will decay to an amplitude less than its arbitrarily small initial value, it can be concluded that the velocity disturbance will not grow in time. Therefore, for values of the parameter $a\eta p_0/b\rho cAT_0$ less than one, the homogeneous straining motion may be considered stable.

Typical stable behavior of w_n is exhibited in Fig. 2. The value of $\frac{\rho Ac^2T_0^2b}{\eta^2a^2\dot{\varepsilon}_0^2l^2}$ is taken to be one, and $a\eta p_0/b\rho cAT_0$ is taken to be 0.5. Results for components with $n = 1$, 5 and 10 are plotted.

For values of the parameter $a\eta p_0/b\rho cAT_0$ greater than one, components of the perturbed velocity field are found to grow in time, reaching final stationary values that are generally much larger than their initial values. Larger values of k_n, corresponding to larger n, result in larger final stationary values of w_n. As the components grow, eventually the small perturbation assumption made in the analysis no longer holds. Therefore, the present analysis simply indicates that the motion of the fiber will tend to deviate initially from homogeneous straining at some point in the extension process for which the parameter value becomes greater than one. We denote $a\eta p_0/b\rho cAT_0$ as the *strain localization parameter*, or SLP.

3. Experiments

A commercial nylon filament, about 140 μm in diameter, sold for use as monofilament sewing thread, was investigated. Filament specimens, nominally 60 mm long, were extended to break at a strain rate of 0.0015 s^{-1} using an Instron test machine, and at a strain rate of about 70 s^{-1} using a simple drop weight test device. Here we will refer to the 0.0015 s^{-1} strain rate extension tests as the "low-rate" tests and the 70 s^{-1} strain rate extension tests as the "high-rate" tests.

A simple drop weight test device was used for the high rate tests. The nylon filament specimen is attached to a load cell (Entran Model ELFS-T3E-250N) at the end of guide tube. A large clamp is attached to the lower end of the specimen. A massive falling

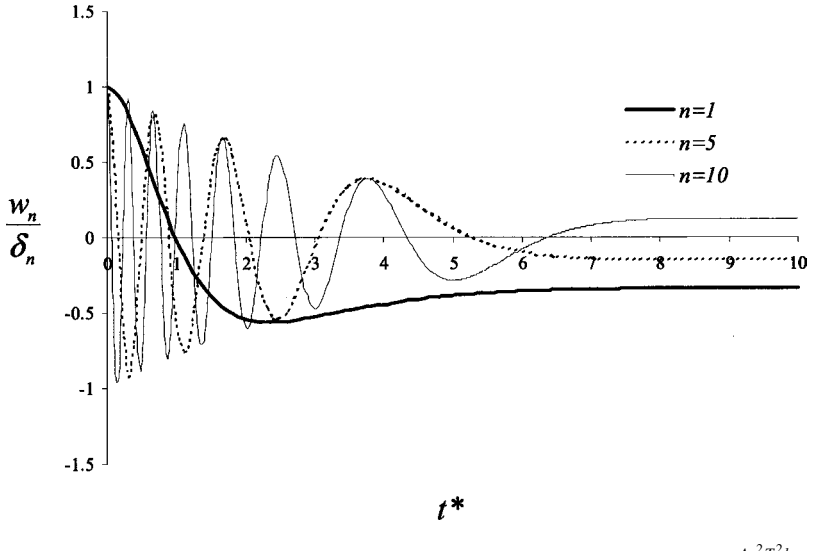

Figure 2 Typical stable behavior of components of the perturbed velocity field, w_n. Results shown here are for $\frac{\rho Ac^2T_0^2b}{\eta^2a^2\dot{\varepsilon}_0^2l^2} = 1, a\eta p_0/b\rho cAT_0 = 0.5$.

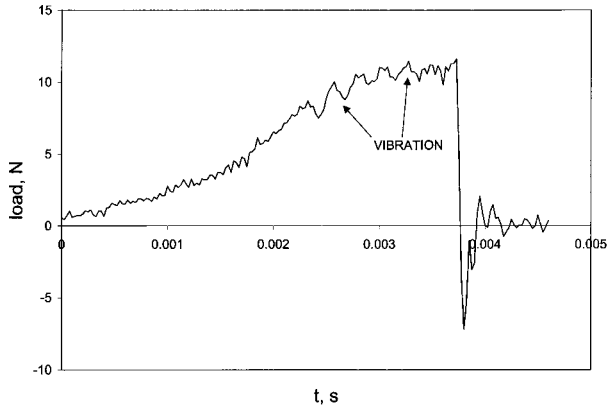

Figure 3 Typical load cell response in high rate extension test.

weight impacts the clamp, extending the specimen with a nearly constant end velocity of 4.2 m s^{-1}. The load cell response is sampled at 40 kHz, as exhibited for a typical test in Fig. 3.

The load cell/filament specimen connection was made as lightweight as possible to minimize the effect of added sprung mass on the dynamic response of the load cell. To form an end termination of the filament specimen, the filament was wrapped around a metal eye and secured with epoxy (typical mass of eye/epoxy: 0.3 g). The eye was attached to a lightweight hook (2.4 g) threaded onto the load cell stud. The natural frequency of the load cell/hook/eye system has been found to be 4,500 Hz. A 4,500 Hz vibration can be seen in the response curve in Fig. 3 in the later stages of specimen extension and after specimen failure. The vibration masks the true magnitude of the filament load as a function of time, however, the response can still be used to accurately determine the elongation-to-break.

Typical high-rate and low-rate load-elongation curves are exhibited in Fig. 4. The load-time series data from the high-rate tests was converted to load-elongation series data by computing the displacement of the specimen end based on the elapsed time after impact and the velocity of the falling weight and subsequently dividing the end displacement by the specimen gage length. It can be seen that specimen breaks at a

TABLE I Elongation-to-break (%) for 60 mm nylon filaments

High-rate tests	18.99
	22.12
	24.27
	24.49
	25.34
	25.75
	26.90
	28.07
	28.42
Low-rate tests	28.21
	30.02
	31.2
	31.5
	31.67
	31.85
	32.05
	32.24
	32.24
	33.38
	33.9
	37.54

lower elongation in the high-rate test as compared with the low-rate test.

Elongation-to-break results for the high-rate and low-rate tests are presented in Table I. For consistency, in the high-rate tests, the elongation-to-break was defined as the first elongation data point recorded *during the load drop* associated with failure. The experimental distributions for elongation-to-break in the high-rate and low-rate tests are plotted in Fig. 5. It can be seen that there is very little overlap in the distributions. As expected, applying the Smirnov test [4], the hypothesis that the high and low rate sample distributions come from the same population is rejected at the 0.01 significance level.

To determine the elongation at which plastic deformation initiates in extension of the nylon filament, a series of tests were performed in which specimens were extended to a prescribed maximum elongation and then slowly unloaded back down to zero elongation (original gage length). After allowing specimens to rest overnight, measurements were made of specimen length to determine the presence of permanent set. It was found that plastic deformation set in at about 12% elongation.

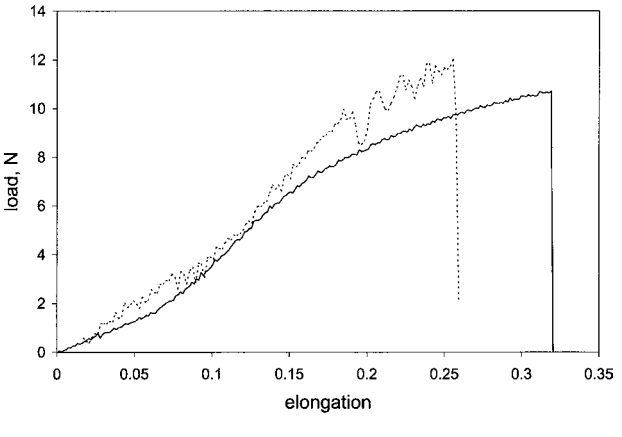

Figure 4 Typical low rate (solid line) and high rate (dotted line) load-elongation curves.

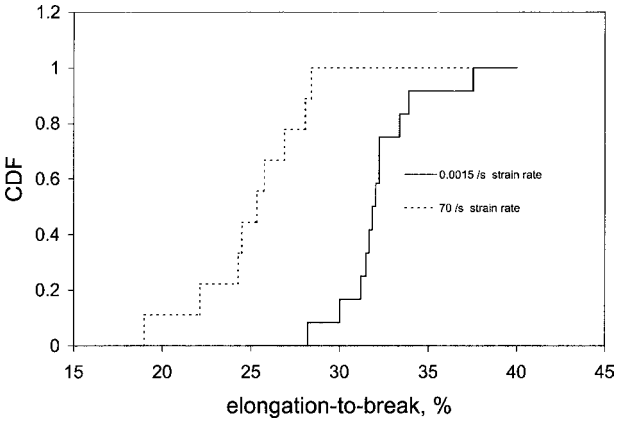

Figure 5 Experimental cumulative distribution functions for elongation-to-break in low rate (solid line) and high rate (dotted line) extension tests.

4. Discussion

The stability analysis has shown that initially homogeneous adiabatic plastic extension of a textile fiber tends to become non-homogeneous at a point in the process where the strain localization parameter attains a value greater than one. As the non-homogeneity develops, strain will become increasingly localized into a region(s) of locally higher temperature, instead of uniformly distributed along the filament. While the present analysis applies only to the initial period of localization, it is likely that after this initial phase, strain localization will continue to grow more pronounced with continued extension. Typically in localization phenomena, regions of increasing deformation become contained in narrow bands, as elastic unloading occurs outside the bands [5]. Elastic unloading was not included in the present model, as it would not occur in the initial development of the localization. Strain energy released by elastic unloading provides an additional energy source driving further plastic deformation within the strain localization band, promoting further localization. Physical reasoning suggests that SLP values greater than one indicate the development of a localized straining mode of extension that will persist through to the eventual rupture of the filament within a localization band.

In filament specimens of length far greater than the filament diameter, it is reasonable to expect that the localization band will be a small fraction of the specimen length. Rupture of the specimen should occur soon after the development of the localization band, and the elongation-to-break of the specimen should be very close to the elongation at which strain localization initiates.

In this section, we estimate the value of the SLP as the specimen is extended. For a rough estimate, quantities that may vary 10% or less during extension will be treated as constants, therefore, η will be assigned the value 0.8, consistent with results in [6], and the filament temperature, T_0, which calculations indicate may increase by 20°C during homogenous straining [7], will be assigned the value 297 K (room temperature during the experiments). The mass per unit length of the filament, ρA, was found to be 0.0185 g m^{-1}, and specific heat $c = 1.43$ J g^{-1} K^{-1} for nylon.

To investigate and quantify the thermal softening coefficient, a, elevated temperature (57.5°C) extension tests were done on 60 mm specimens at the 0.0015 s^{-1} strain rate and compared with the room temperature low-rate tests. A hot air blower was used to maintain the filament temperature during the test. Because of the fineness of the filament, thermal equilibrium is reached after seconds of immersion in the hot air flow, so the procedure was to turn on the hot air blower and immediately begin the extension test. It turns out that the elevated temperature curves are shifted downward to a lower load by a nearly constant value of 2.5 N for elongations greater than about 14%. Using Equation 2 and the temperature change of 33.5°C, a was determined to have a constant value of 22 N.

The other constitutive parameters, p_0 and b, can vary greatly during the extension process, as can be seen in Fig. 4. The parameter b is essentially the slope of the load-elongation curve. In Fig. 6, b is estimated from a typical low rate test. The value of b is seen to vary from over 60 N at the onset of plastic extension to about 14 N at filament rupture. The parameter p_0, the current value of the plastic load, increases from about 5 N at the beginning of plastic deformation to over 10 N at failure in the low-rate tests.

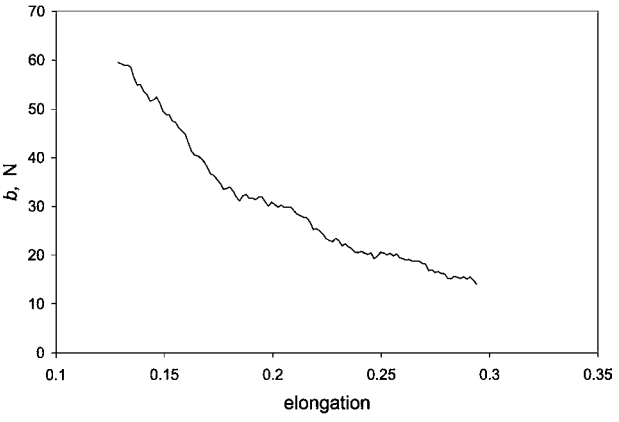

Figure 6 Behavior of parameter b with increasing elongation estimated from a typical low rate load-elongation curve.

The value of the strain localization parameter with increasing elongation is exhibited in Fig. 7, where p_0 and b have been treated as functions of elongation. The estimates were calculated based on five typical low-rate load-extension curves. At the beginning of plastic extension, the estimated value of the strain localization parameter is about 0.18. The value of the SLP steadily increases with increasing extension, attaining a value of one at elongations ranging from 0.23 to 0.27.

As the nylon filament is plastically extended at a high rate, the SLP is initially well below the threshold required for the strain localization process to be triggered. Therefore, for some time, we expect that the filament will extend more or less homogenously. A point is reached, however, when the current value of the plastic load becomes sufficiently high, and the strain hardening coefficient becomes sufficiently low, that the SLP attains values of one or greater. The strain localization process begins and localization bands rapidly develop, the initial process being further reinforced by elastic

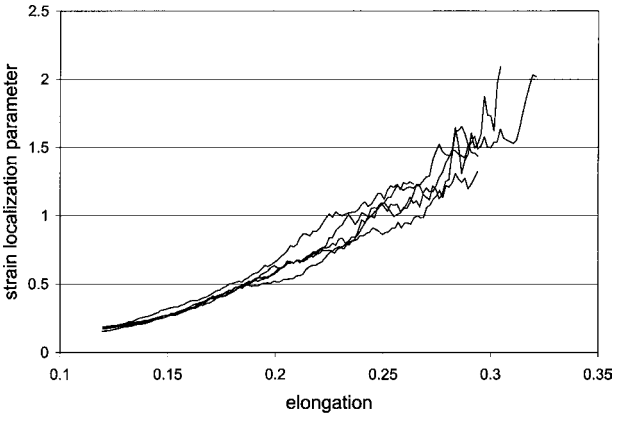

Figure 7 Behavior of SLP with increasing elongation determined from five typical low rate load-elongation curves.

unloading in the filament outside the developing localization bands. Recalling the argument given earlier in this section, the likely size of the bands being many orders of magnitude less than the filament specimen length, the elongation-to-break may be expected to be approximately equal to the elongation at the onset of localization.

The estimates for elongation values corresponding to the onset of strain localization in high-rate extension, falling in the range of 0.23 to 0.27, compare favorably with the high-rate elongation-to-break results (mean: 0.25) given in Table I. The good agreement between the estimated elongation at onset of localization and the experimental high rate elongation-to-break results supports the above interpretation of the localization and failure process, and corroborates the stability analysis.

5. Conclusions

A stability analysis of homogeneous straining motion in the adiabatic high-rate extension of textile fibers has been presented. For particular values of a *strain localization parameter* (SLP) involving constitutive and thermo-physical properties of the fiber, it was shown that initially homogeneous straining motion of the fiber tends to become non-homogeneous (localized) with continued extension. Physical reasoning was given suggesting that, once begun, strain localization intensifies and persists with increasing extension to the point of final filament rupture. High-rate and low-rate extension experiments on nylon filaments were presented that exhibited reduced elongation-to-break at the high-strain rate, consistent with predictions made using the SLP of the occurrence of localized, versus uniform, straining. In addition, the transition from homogeneous to localized straining was shown to occur at elongations that correspond with the SLP attaining a critical value for onset of localization.

References

1. G. HOLDEN, *J. Textile Inst.* **50** (1959) T41.
2. T. A. GODFREY, *Textile Res. J.* **70** (2000) 646.
3. J. C. SMITH, P. J. SHOUSE, J. M. BLANDFORD and K. M. TOWNE, *ibid.* **31** (1961) 721.
4. B. W. LINDGREN and G. W. McELRATH, "Introduction to Probability and Statistics" (The Macmillan Company, New York, 1959) p. 204.
5. Z. P. BAZANT and L. CEDOLIN, "Stability of Structures" (Oxford University Press, New York, 1991) p. 845.
6. M. C. BOYCE, E. L. MONTAGUT and A. S. ARGON, *Polym. Eng. Sci.* **32** (1992) 1073.
7. T. A. GODFREY, *J. Textile Inst.* **92** (2001) 16.

Received 13 March
and accepted 29 July 2003